

Supporting Information for
Clustering-Enhanced, Nonconventional Photoluminescence from
Silicone Surfactant

Aoxue Xu,^aHailong Liu,^b Gang Yi,^b Ning Feng,^a and Hongguang Li^{a,*}

^a Key Laboratory of Colloid and Interface Chemistry, Ministry of education, School of Chemistry and Chemical Engineering, Shandong University, Jinan, 250100, China

^b Shandong Key Laboratory of Advanced Organosilicon Materials and Technologies, Zibo, 256401, China

Corresponding Author

hgli@sdu.edu.cn

Tel: +86-531-88363963

Fax: +86-531-88364750

1. Experimental section

1.1 Materials

The silicone surfactant, (polyether trisiloxane, 1,1,1,3,5,5,5-Heptamethyl-3-(3-poly(ethyleneoxide) propyl) trisiloxane, abbreviated to PTS hereafter), was bought from Dongyue Silicone Materials Co., Ltd., which was delivered as a viscous fluid with a viscosity of ~ 39.4 mPa·s. The content of Pt (from catalyst) was probed by inductively coupled plasma mass spectrometer, which is 2.65 mg·L⁻¹. Sodium dodecyl sulphate (SDS, 99%) was purchased from Sinopharm Chemical Reagent Co., Ltd. The nonionic surfactant used for comparison (Triton X-100) was purchased from Sigma. These chemicals were used without further purification. Ultrapure water used in the experiments with a resistivity of 18.25 M Ω cm⁻¹ was obtained using a UPH-IV ultrapure water purifier (China).

2.2 Sample preparation methods

Samples of PTS/H₂O binary system were prepared by adding 1.0120 g H₂O to each vial, followed by the addition of desired amount of PTS. The weight percentage of PTS was set between 10 wt% and 80 wt%, with an increment of 10 wt% between adjacent samples. After the samples were homogenized by PTS, they were left at 25 °C for phase equilibrium. Phase sequence was recorded one week after preparation.

Samples of PTS/SDS/H₂O ternary system were prepared by fixing the weight percentage of PTS to water at 10 % while varying the molar ratio of SDS to PTS ($n_{\text{SDS}}/n_{\text{PTS}}$). Take the series with $n_{\text{SDS}}/n_{\text{PTS}}$ of 1.5 for example, first an aqueous stock solution of SDS with a weight percentage of 30% was prepared. Then, 2.6257 g SDS stock solution and 1.1515 g PTS were added to a vial, followed by the addition of 8.5250 g H₂O. The samples were homogenized by PTS and left at 25 °C for phase equilibrium. Phase sequence was recorded one week after preparation, while optical measurements were performed at least three months later. We also carried out time-dependent PL measurements on

the PTS/SDS/H₂O ternary system.

2.3 Methods

Nuclear magnetic resonance (NMR) spectra were obtained from a 400 MHz nuclear magnetic resonance (Switzerland Bruker). The residual Pt involved in PTS was detected by inductively coupled plasma mass spectrometer (NexION 350X, Perkin Elmer). Fluorescence spectra were obtained by a spectrofluorometer (FluoroMax-4, Horiba). UV-vis measurements were carried out on a UV-vis-NIR spectrometer (UV-1800, Shimadzu). The absolute fluorescence quantum yield (Φ) and fluorescence lifetime (τ) were measured with a spectrofluorometer (FLSP920, Edinburgh Instruments LTD).

Surface tension measurements were performed using the plate method with a surface tension meter (Germany Biolin Scientific). Rheological measurements were carried out on an Anton-Paar Physica MCR302 rheometer with a cone-plate system. Before the frequency sweep, an amplitude sweep at a fixed frequency of 1 Hz was carried out to ensure that the selected stress was in the linear viscoelastic region. The frequency sweep was carried out from 0.01 to 100 Hz at a fixed stress of 10 Pa.

For cryo-TEM tests, the sample ($\sim 4 \mu\text{L}$) was dropped onto a micro grid under high humidity ($>80\%$). Excess sample was removed with two pieces of filter paper, leaving a thin film sprawling on the micro grid, which was plunged into liquid ethane pre-liquefied with liquid nitrogen. The vitrified sample was transferred into a sample holder (Gatan 626) and observed on a JEOL JEM-1400 TEM (120 kV) at $\sim -174 \text{ }^\circ\text{C}$. The images were recorded on a Gatan multiscan CCD. To get solid conclusions, observations were carried out on the microscopes located both in Shandong University (Jinan, Shandong Province, China) and China University of Petroleum (Qingdao, Shandong Province, China).

For freeze-fracture TEM observations, a small amount of sample ($\sim 4 \mu\text{L}$) was dropped on the specimen carrier. The sample was frozen by plunging into liquid propane cooled by liquid nitrogen.

Fracturing and replication were carried out using a freeze-fracture apparatus (EM BAF 060, Leica, Germany) at a temperature of -160 °C. Pt/C was deposited at an angle of 45° to shadow the fracture surface, and C was deposited at an angle of 90° to consolidate the fracture surface. The replicas were transferred onto a copper grid and then checked using a JEOL JEM-1400 TEM (Japan) at an accelerating voltage of 120 kV.

2.4 Calculations based on Gibbs adsorption theory

According to the Gibbs adsorption formula, the maximum adsorption capacity (Γ_{max}) of the surfactant at the gas-liquid interface was calculated using the following equation:¹⁻⁶

$$\Gamma_{max} = - \left(\frac{1}{2.303nRT} \right) \left(\frac{d\gamma}{dlgc} \right) \quad (1)$$

where R is the gas constant (8.314 J·mol⁻¹·K⁻¹), T is the absolute temperature (298.15 K), and (dγ/dlg c) is the slope of the surface tension γ plotted against the lg c below the *cmc*. In current system, n was set as 1 for PTS while 2 for SDS.

The minimum surface area occupied by a single surfactant (A_{min}) can be obtained by:^{1-4,6}

$$A_{min} = \frac{1}{\Gamma_{max} N_A} \quad (2)$$

where Γ_{max} is the maximum adsorption and N_A is the Avogadro constant (6.022×10^{23}).

The free energy of adsorption (ΔG_{ads}) can be calculated using the following formula:^{1,2,4-6}

$$\Delta G_{ads} = RT \ln \frac{c_{\Pi}}{55.5} - 6.022 \Pi A_{min} \quad (3)$$

where Π ($= \gamma_0 - \gamma$) is surface pressure in the region of surface saturation and c_{Π} is the concentration of the surfactant in the aqueous phase at a surface pressure Π (mN·m⁻¹). A is the surface area occupied by a single surfactant at surface pressure Π .

The micellar free energy (ΔG_{mic}) can be calculated using the following formula:^{1,2,4-6}

$$\Delta G_{mic} = RT \ln \left(\frac{cmc}{55.5} \right) \quad (4)$$

2. Additional data

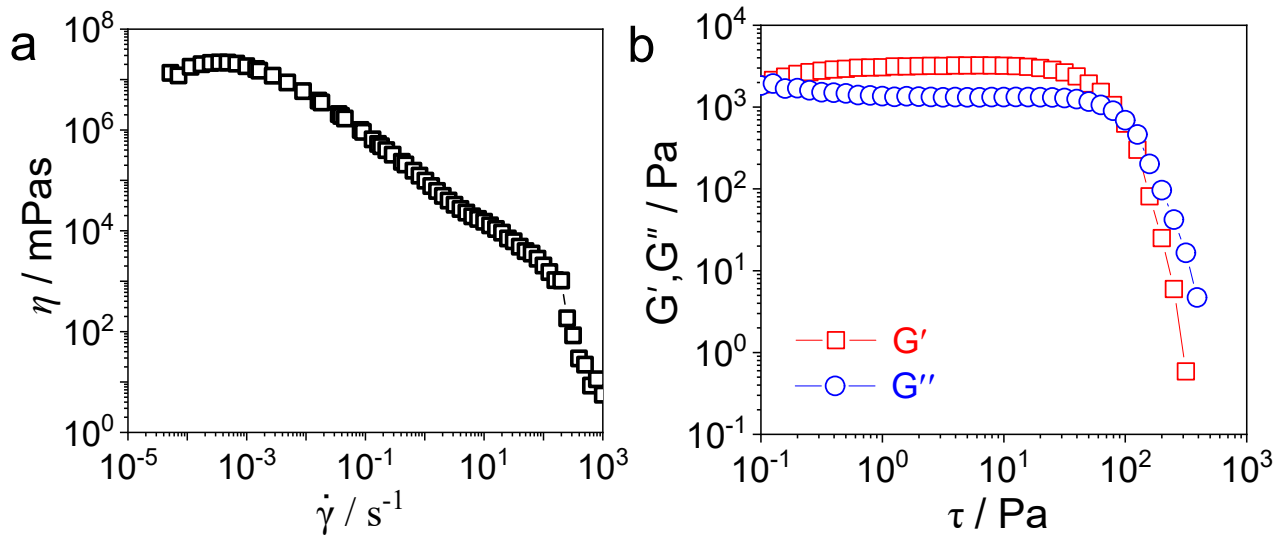


Fig. S1 (a) Variation of viscosity as a function of shear rate and (b) Variation of elastic modulus, viscous modulus and complex viscosity as a function of the stress for the sample with c_{PTS} of 10 wt% and n_{SDS}/n_{PTS} of 8.5.

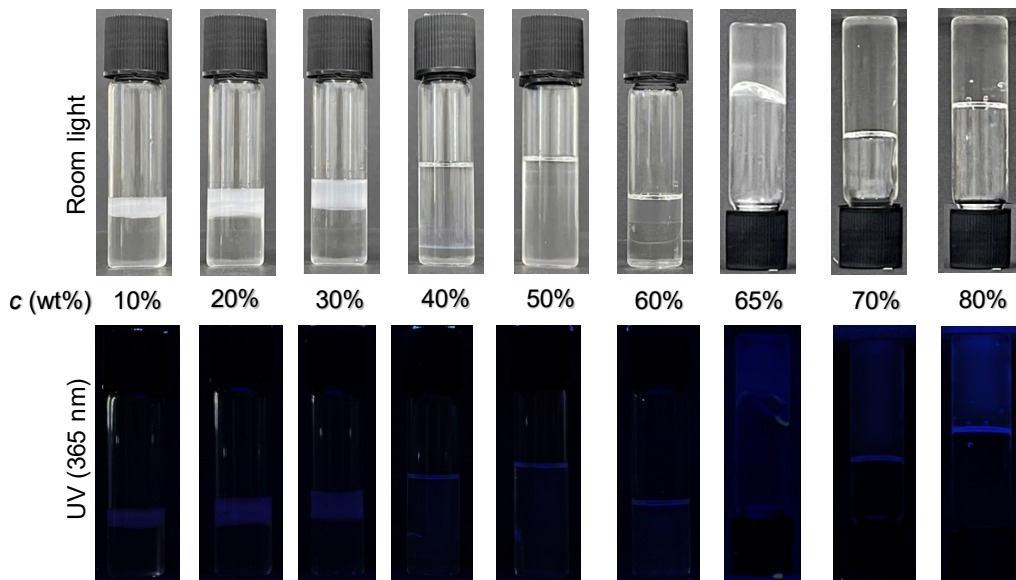


Fig. S2 Photos of samples in the PTS/H₂O binary system with varying concentrations as indicated, taken under room light and 365 nm UV irradiation, respectively.

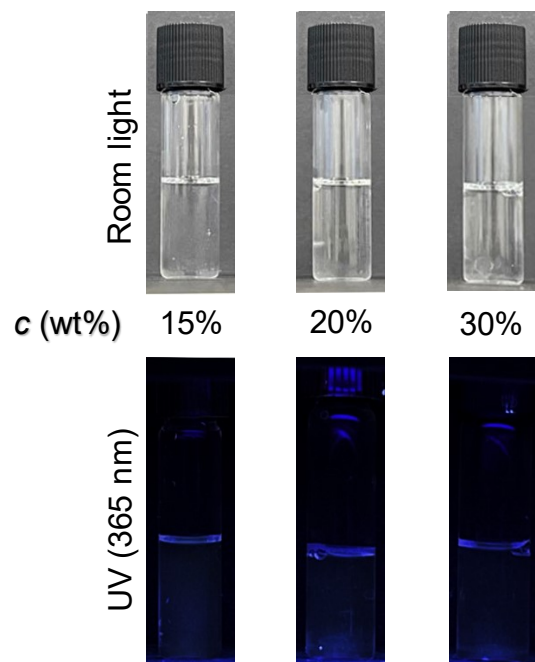


Fig. S3 Photos of three SDS aqueous solutions with different concentrations as indicated, taken under room light and 365 nm UV irradiation, respectively. The PL is negligible.

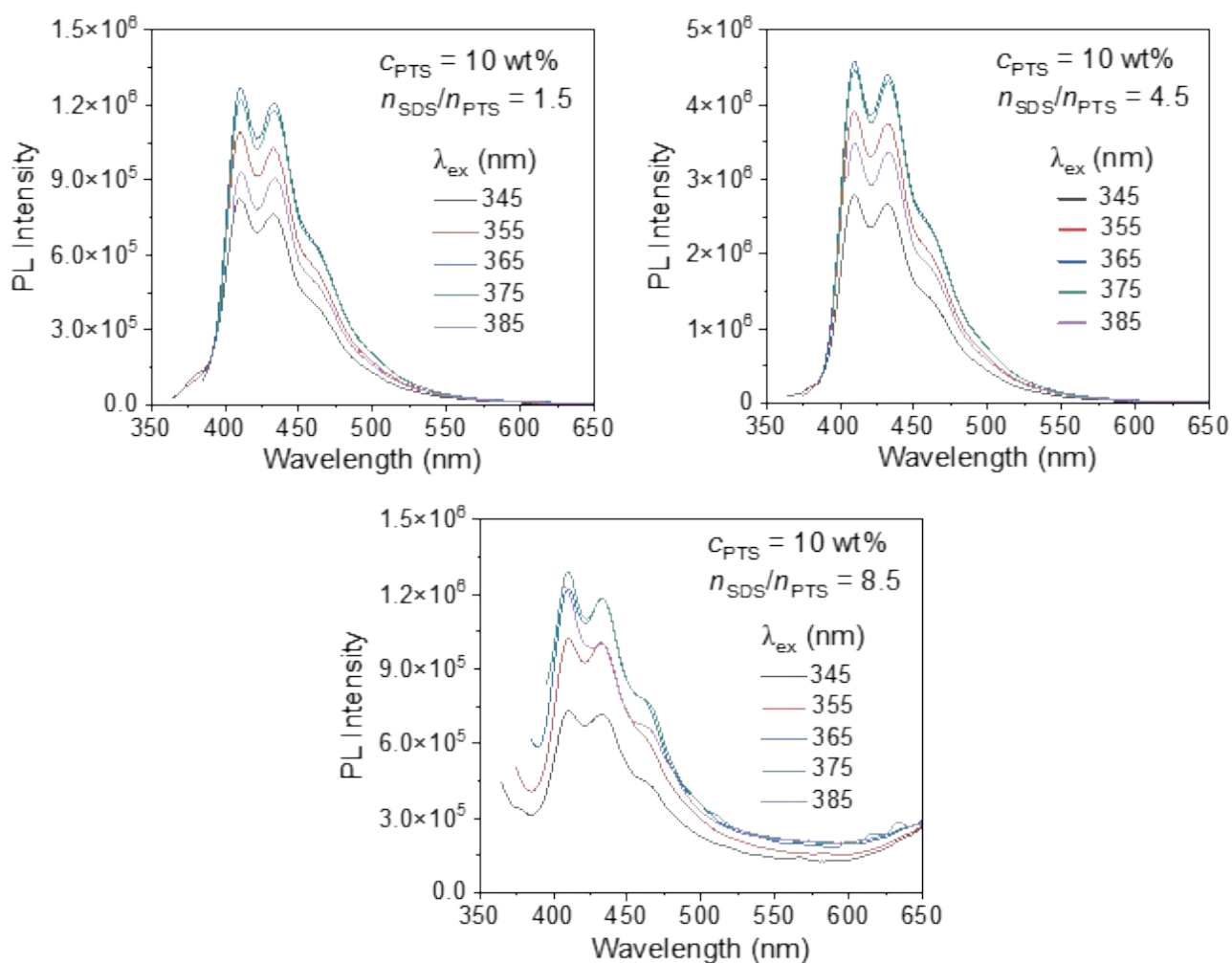


Fig. S4 Emission spectra recorded at varying excitation wavelength of three typical samples from SDS/PTS/H₂O ternary system with different compositions as indicated.

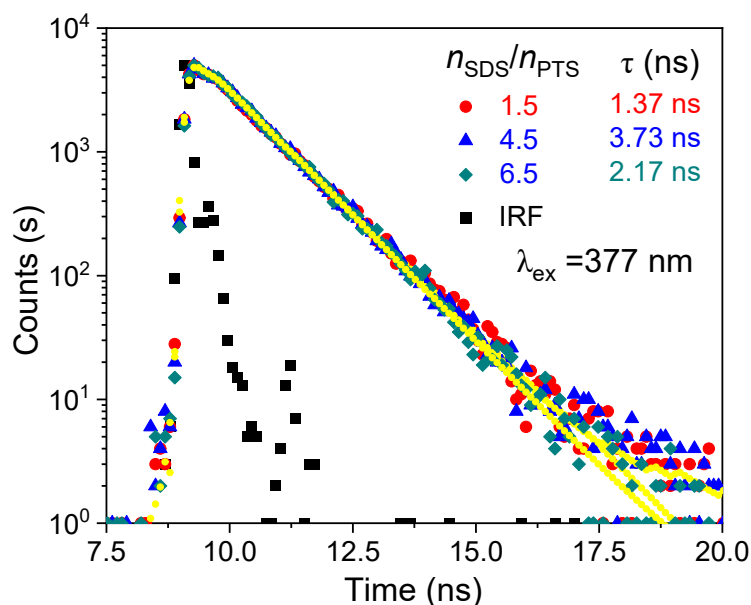


Fig. S5 PL decay profiles under 377 nm excitation of the samples with $c_{\text{PTS}} = 10$ wt% and varying $n_{\text{SDS}}/n_{\text{PTS}}$ as indicated.

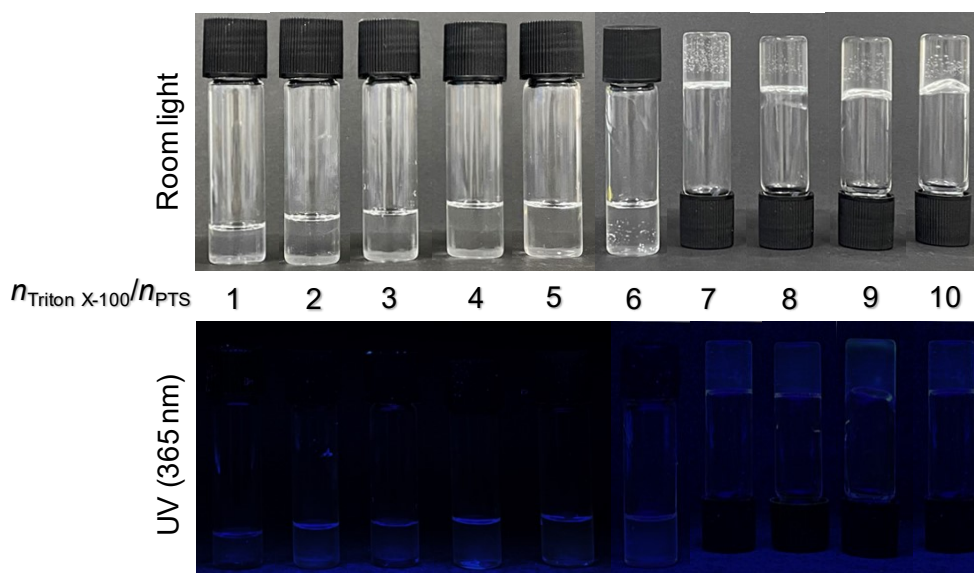
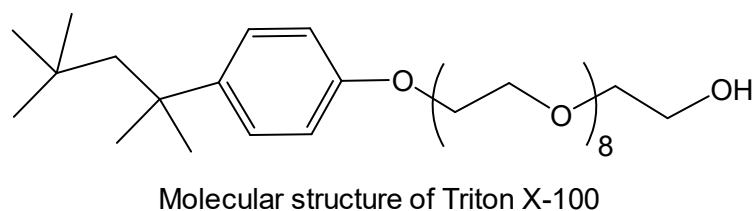


Fig. S6 Photos of samples in the Triton X-100/PTS/H₂O ternary system with varying molar ratio of Triton X-100 to PTS as indicated, taken under room light and 365 nm UV irradiation, respectively.

Notion: From the molecular structure of Triton X-100, one can see that it contains a phenyl group. Thus, strictly speaking, its PL is not merely n-PL. Despite of the presence of this phenyl group, the combination of Triton X-100 and PTS did not lead to strong PL enhancement, which is in contrast of the SDS/PTS combination presented in the maintext. This observation highlighted the advantage of the SDS/PTS combination in enhancing the n-PL.

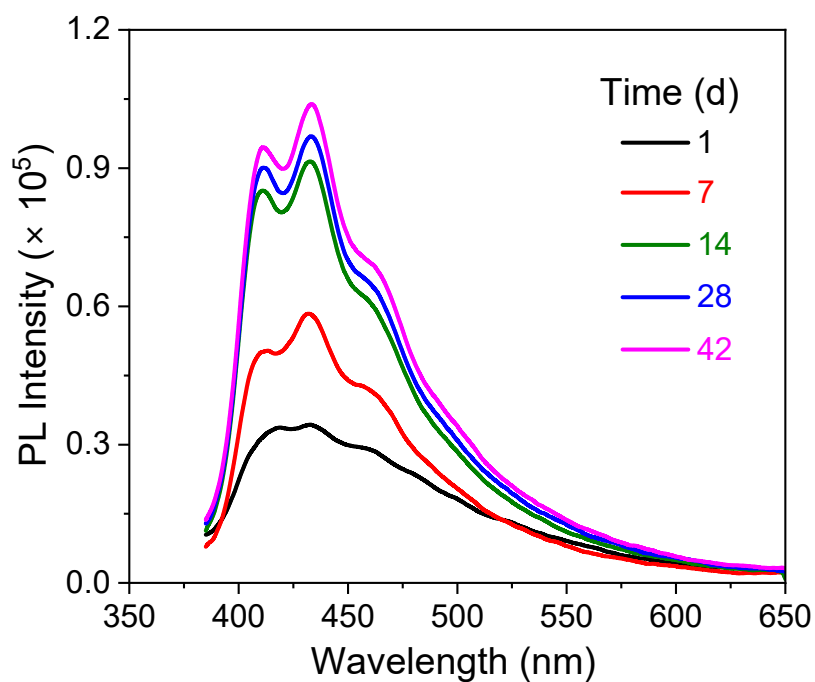


Fig. S7 Evolution of the emission at 365 nm excitation of the sample with $c_{\text{PTS}} = 10$ wt% and $n_{\text{SDS}}/n_{\text{PTS}} = 1.5$.

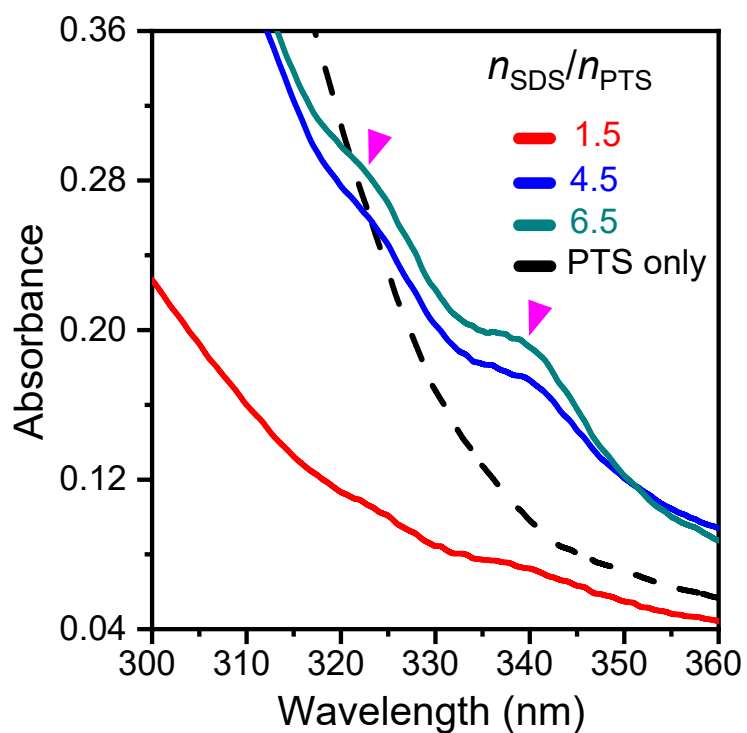


Fig. S8 Enlarged UV-vis absorption (the same curves as those in Fig. 3c in the maintext) of typical samples from the SDS/PTS/ H_2O ternary system with 10 wt% PTS and varying $n_{\text{SDS}}/n_{\text{PTS}}$.

3. Tables and Schemes

Table S1. Summary of typical organic materials exhibiting *n*-PL reported in recent years.

Name (physical state) ^a	Color	Φ (%) ^b	Reference
Hyperbranched and linear polyethylenimines (<i>s</i>)	Blue	1.0~20.0 (R)	<i>Macromol. Rapid Commun.</i> , 2007 , 28, 1404-1409.
Aliphatic biodegradable photoluminescent polymers (<i>s</i>)	Blue/red	0.4~62.3 (R)	<i>Acad. Sci.</i> , 2009 , 106, 10086-10091.
Linear poly ethylenimines (<i>s</i>)	Blue	2.0 (R)	<i>Chem. Commun.</i> , 2010 , 46, 5554-5556.
Aliphatic hyperbranched poly (amido acids) (<i>s</i>)	Blue	23 (R)	<i>Polymer</i> , 2013 , 54, 623-630.
Poly [(maleic anhydride)-alt-(vinyl acetate)] (<i>s</i>)	Blue, Green, Red	~ 20 (R)	<i>Macromolecules</i> , 2015 , 48, 64-71.
Non-conjugated polyacrylonitrile (<i>p</i>)	Blue	16.9 (A)	<i>Small</i> , 2016 , 12, 6586-6592.
Aliphatic hyperbranched poly ether (<i>s</i>)	Blue	11~39 (R)	<i>Phys. Chem. Chem. Phys.</i> , 2016 , 18, 4295-4299.
Hyperbranched poly carbonate (<i>f</i>)	Blue	7.4~8.4 (A)	<i>J. Polym. Sci., Part A: Polym. Chem.</i> , 2017 , 55, 3690-3696.
Hyperbranched poly esters (<i>f</i>)	Blue	16.8 (A)	<i>ACS Sustainable Chem. Eng.</i> , 2017 , 5, 6139-6147.
Poly (maleic anhydride-alt-vinylpyrrolidone) (<i>p</i>)	Yellow/White	0.1~24.6 (A)	<i>J. Mater. Chem. C</i> , 2017 , 5, 8082-8090.
Nonaromatic poly urethanes (<i>p</i>)	Blue/Green	6.2~13.1 (A)	<i>Mol. Syst. Des. Eng.</i> , 2018 , 3, 364-375.
Hyperbranched poly (amino ester) s (<i>f</i>)	Blue	1.1~8.7 (A)	<i>Macromol. Rapid Commun.</i> , 2019 , 40, 1800658-1800663.
Sulphur-containing linear nonaromatic polymers (<i>p</i>)	Blue	4.5~12.8 (A)	<i>Polym. Chem.</i> , 2019 , 10, 3639-3646.
Poly(ethylene glycol) and lipoic acid modified poly(isobutylene-alt-maleic anhydride) (<i>s</i>)	Blue	/	<i>Bioconjugate Chem.</i> , 2019 , 30, 871-880
Azido substituted poly (vinylidene fluoride) (<i>s/flm</i>)	Blue	0.8~10.3 (R)	<i>Polym. Chem.</i> , 2020 , 11, 1307-1313.
Hyperbranched poly borate (<i>f</i>)	Blue	54.1 (A)	<i>Angew. Chem. Int. Ed.</i> , 2022 , 61, e202204383.

Table S1. (continued)

Linear non-conjugated polyester (<i>p</i>)	yellowish-green	38 (A)	<i>Angew. Chem. Int. Ed.</i> , 2022 , 61, e202114117.
poly(maleimide)s (<i>p</i>)	Multi-color	1.2-16.2 (not mentioned)	<i>Nat. Commun.</i> , 2022 , 13, 3717.
succinimide derived cyclic imides (<i>c</i>)	Orange/ Red	4.2-16.6 (A)	<i>Nat. Commun.</i> , 2022 , 13, 2658.
amino acid-constructed polyureas (<i>s</i>)	Blue/Green	29 (R)	<i>Nat. Commun.</i> , 2022 , 13, 4551.
Copolymers (<i>s</i>)	Blue	2.3-8.2 (A)	<i>Macromolecules</i> , 2022 , 55, 8599-8608.
Milk powder (<i>s/p</i>)	cyan	5.3-25.7 (A)	<i>J. Mater. Chem. C</i> , 2022 , 10, 15629-15637.

^a *s*: solution. *p*: powder. *f*: solvent-free fluid. *c*: crystal.

^b R: Relative Φ . A: Absolute Φ .

Table S2. Summary of Silicone-based organic materials exhibiting *n*-PL reported in recent years. The structures can be found in Scheme S1-S4.

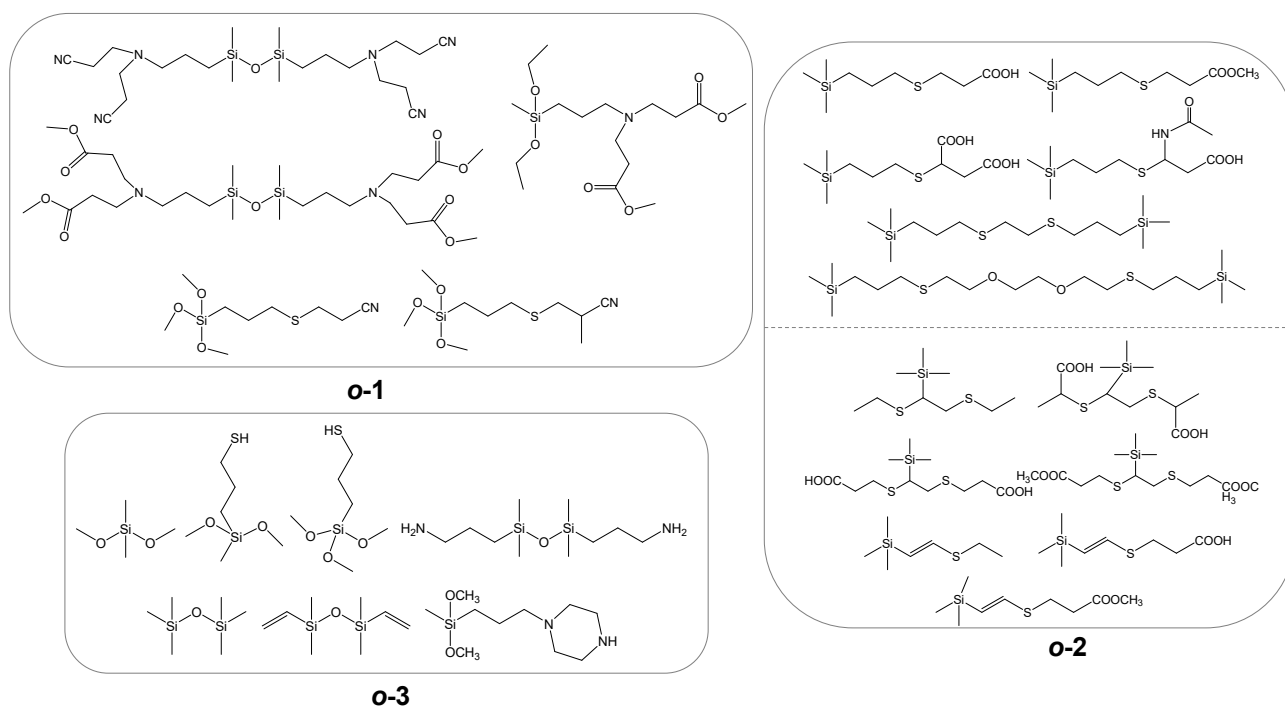
Type	Number	color	Φ (%)	Reference
Oligo-	<i>o</i> -1 (<i>s</i>)	Blue	0.010-0.067 (R)	<i>Chem. Asian J.</i> , 2017 , <i>12</i> , 1213 - 1217.
	<i>o</i> -2 (<i>s</i>)	Blue	/	<i>ChemistrySelect</i> , 2017 , <i>2</i> , 4376 - 4381.
	<i>o</i> -3 (<i>s</i>)	Blue/red	2.04-4.13 (A)	<i>Adv. Funct. Mater.</i> , 2020 , <i>30</i> , 1910536.
Linear	<i>l</i> -1 (<i>s</i>)	Blue	/	<i>J. Photochem. Photobiol. A</i> , 2018 , <i>350</i> , 152-163.
	<i>l</i> -2 (<i>s</i>)	Blue	23.6 (R)	<i>J. Mater. Chem. C</i> , 2017 , <i>5</i> , 4892-4898.
	<i>l</i> -3 (<i>s</i>)	Blue	/	<i>New J. Chem.</i> , 2017 , <i>41</i> , 14545.
	<i>l</i> -4 (<i>s</i>)	Blue	/	<i>Polymers</i> , 2019 , <i>11</i> , 1235.
	<i>l</i> -5 (<i>f/s</i>)	Blue	4.2 (R)	<i>Polym. J.</i> , 2019 , <i>51</i> , 869-882.
	<i>l</i> -6 (<i>s</i>)	Blue	/	<i>Polym. Chem.</i> , 2020 , <i>11</i> , 4780-4786.
	<i>l</i> -7 (<i>f/s</i>)	Yellow/Blue	2.8 (A)	<i>J. Phys. Chem. B</i> , 2021 , <i>125</i> , 4321-4329.
	<i>h</i> -1 (<i>f</i>)	Blue	/	<i>Macromolecules</i> , 2015 , <i>48</i> , 476-482.
	<i>h</i> -2 (<i>s</i>)	Blue	/	<i>Phys. Chem. Chem. Phys.</i> , 2015 , <i>17</i> , 26783-26789.
	<i>h</i> -3 (<i>f/s</i>)	Blue	/	<i>Macromol. Chem. Phys.</i> , 2016 , <i>217</i> , 1185-1190.
Hyper-branched	<i>h</i> -4 (<i>f</i>)	Blue	/	<i>Macromol. Rapid Commun.</i> , 2016 , <i>37</i> , 318-322.
	<i>h</i> -5 (<i>f/s</i>)	Blue	5.79-11.99 (A)	<i>RSC Adv.</i> , 2016 , <i>6</i> , 106742-106753.
	<i>h</i> -6 (<i>f/s</i>)	Blue	/	<i>Macromol. Rapid Commun.</i> , 2016 , <i>37</i> , 136-142.
	<i>h</i> -7 (<i>p</i>)	Blue	3.7~12.0 (A)	<i>Polym. Chem.</i> , 2016 , <i>7</i> , 3747-3755.
	<i>h</i> -8 (<i>s</i>)	Blue	4.61 (A)	<i>J. Mater. Chem. C</i> , 2016 , <i>4</i> , 6881-6893.

	<i>h</i> -9 (<i>s</i>)	Blue	10.5-43.9 (A)	<i>Macromolecules</i> , 2019 , <i>52</i> , 3075-3082.
	<i>h</i> -10 (<i>s/p</i>)	Blue	12.24-18.72 (A)	<i>Biomacromolecules</i> , 2019 , <i>20</i> , 4230-4240.
	<i>h</i> -11 (<i>s</i>)	Blue	8.8-11.8 (A)	<i>Biomacromolecules</i> , 2020 , <i>21</i> , 3724-3735.
	<i>h</i> -12 (<i>s</i>)	Blue	1.12-7.71 (A)	<i>Mater. Chem. Front.</i> , 2020 , <i>4</i> , 1375-1382.
	<i>h</i> -13 (<i>s</i>)	Blue	23.35-28.57 (A)	<i>Macromol. Chem. Phys.</i> , 2021 , <i>222</i> , 2100283.
	<i>h</i> -14 (<i>s</i>)	Multi-color	19.36-44.84 (A)	<i>Biomacromolecules</i> , 2022 , <i>23</i> , 1041-1051.
	<i>h</i> -15 (<i>s</i>)	Blue	17.88 (A)	<i>Biomaterials Advances</i> , 2022 , <i>137</i> , 212848.
	<i>h</i> -16 (<i>s</i>)	Green, Yellow, Red	3.71-13.87 (A)	<i>Biomacromolecules</i> 2022 , <i>XXXX</i> , <i>XXX</i> , <i>XXX-XXX</i> .
Derivatives of POSS	/ <i>s/p</i>)	Blue	6.9-72.5 (A)	<i>Polym. Chem.</i> , 2016 , <i>7</i> , 135-145.

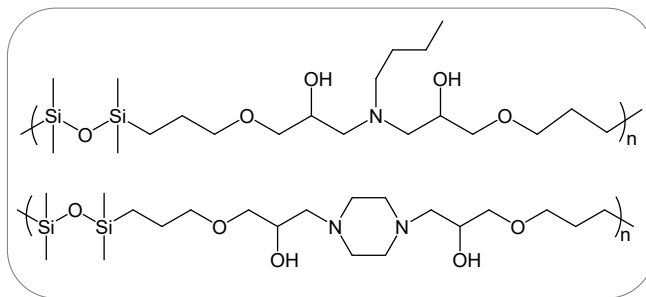
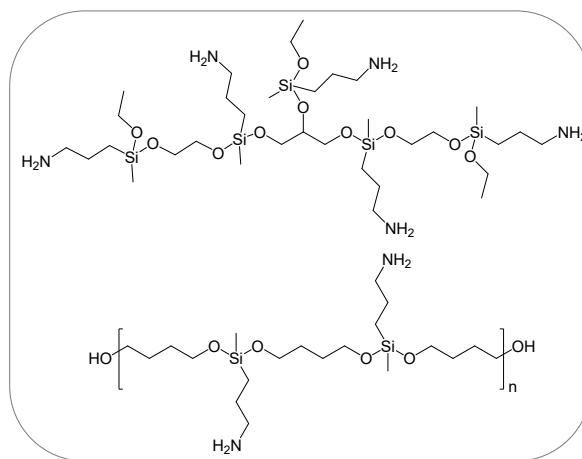
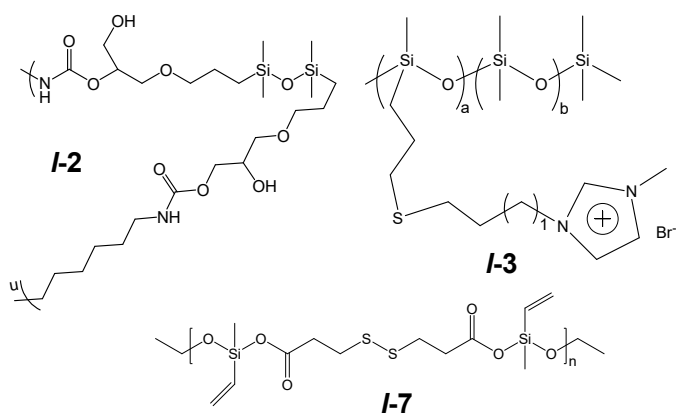
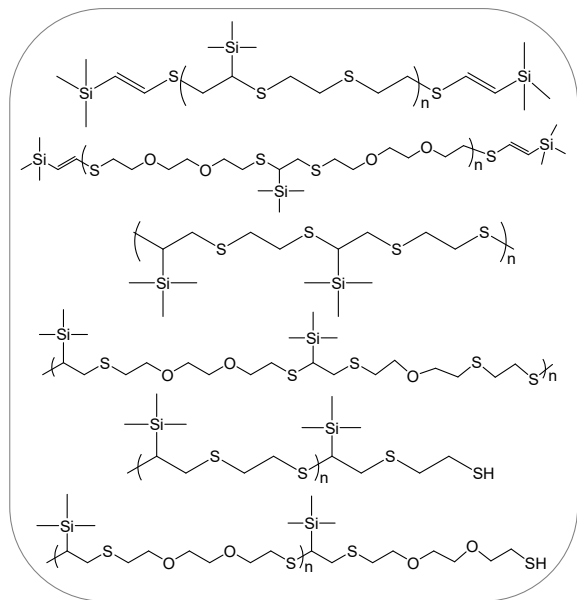
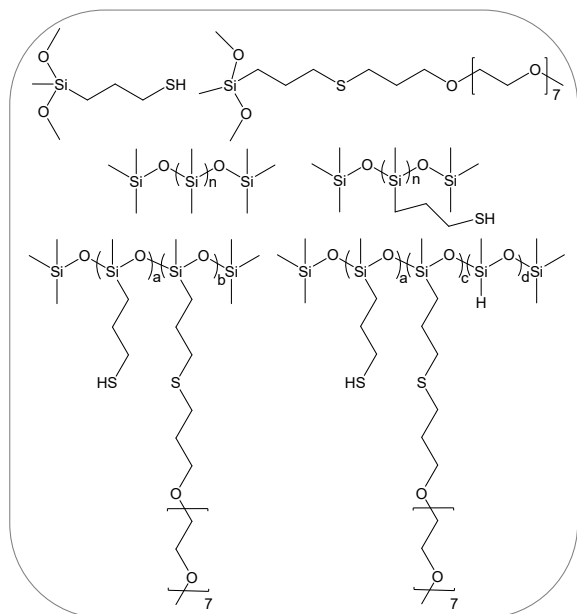
^a *s*: solution. *p*: powder. *f*: solvent-free fluid. *c*: crystal.

^b R: Relative Φ . A: Absolute Φ .

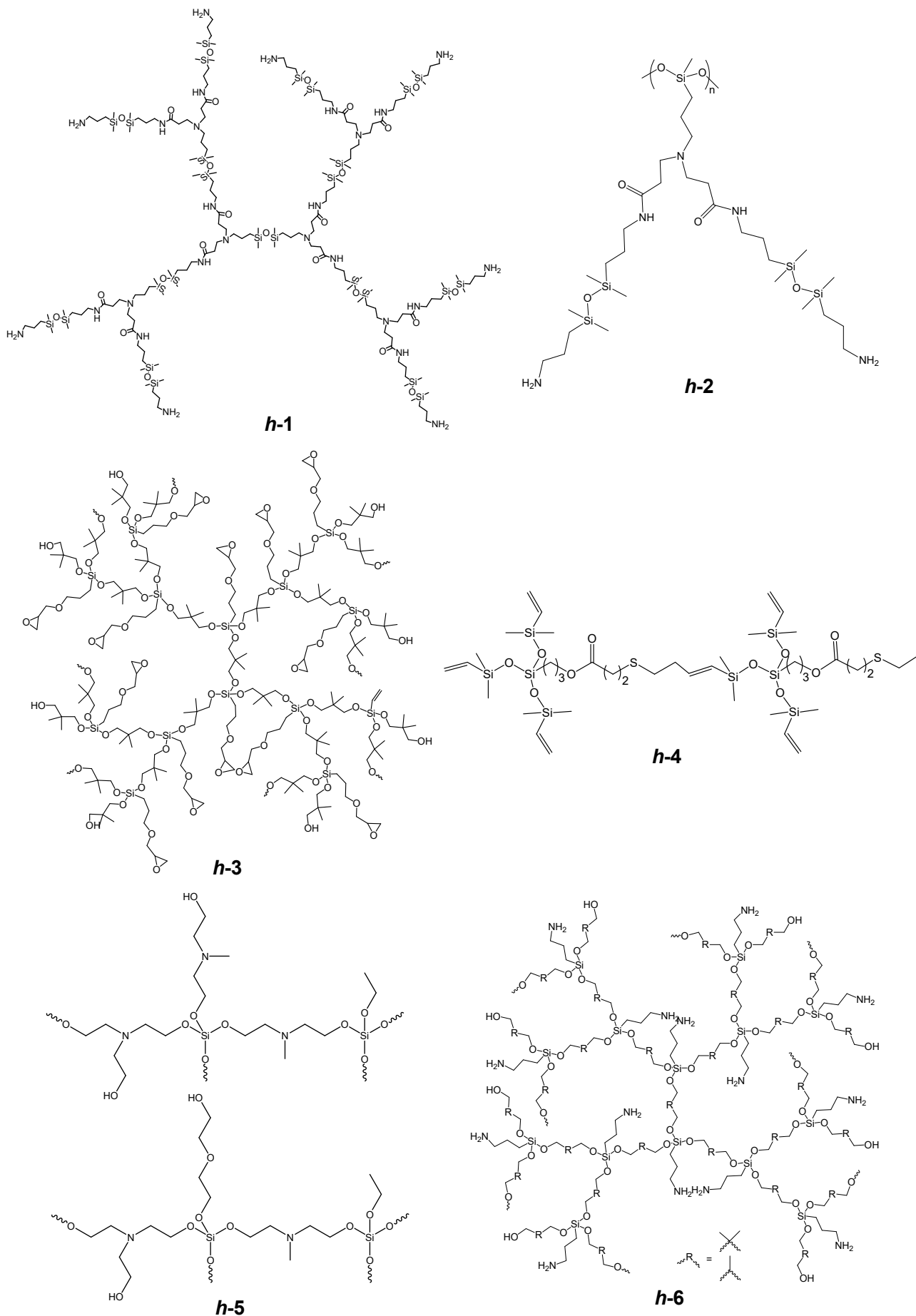
Scheme S1. Structures of the oligo-silicones (*o*-1 to *o*-3).



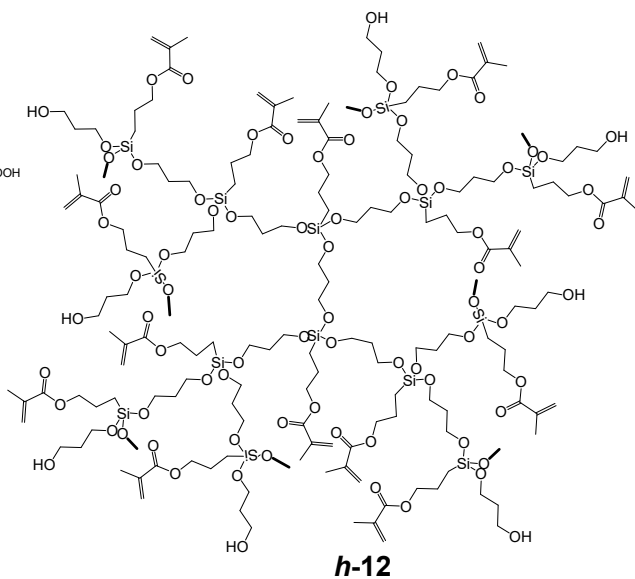
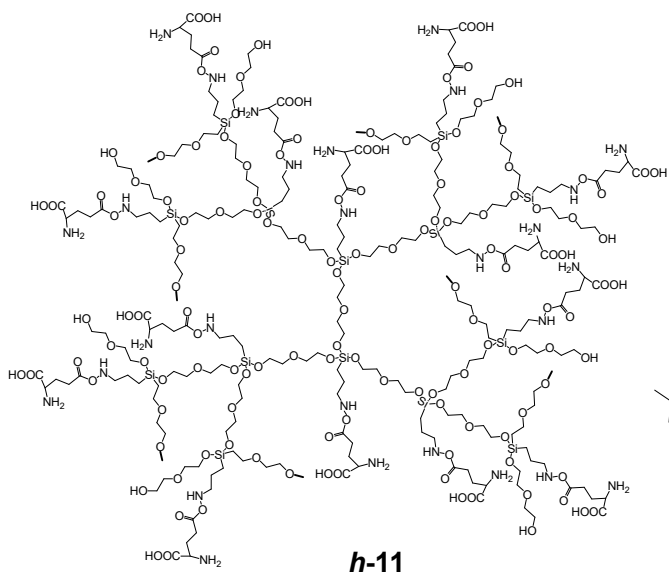
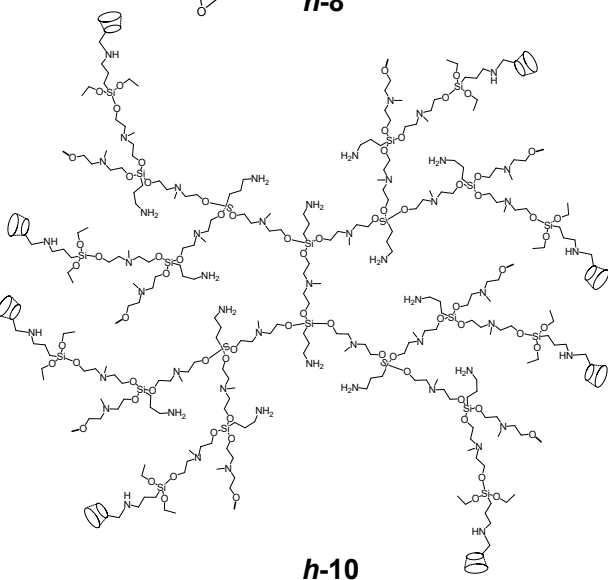
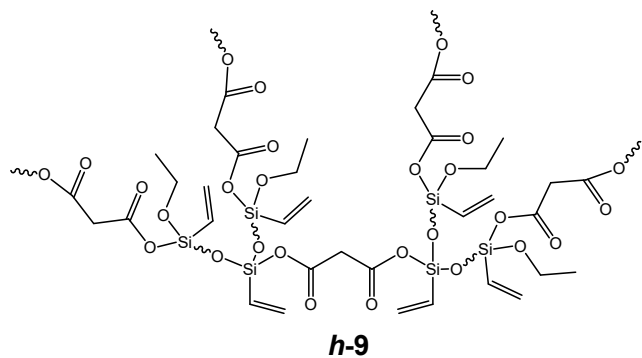
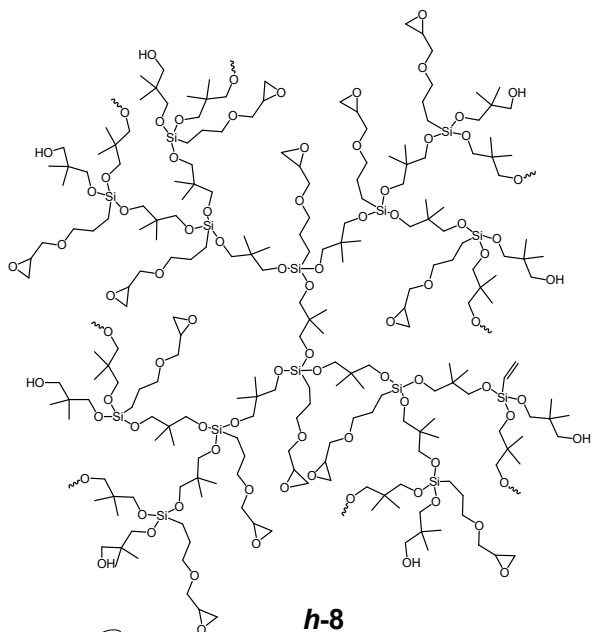
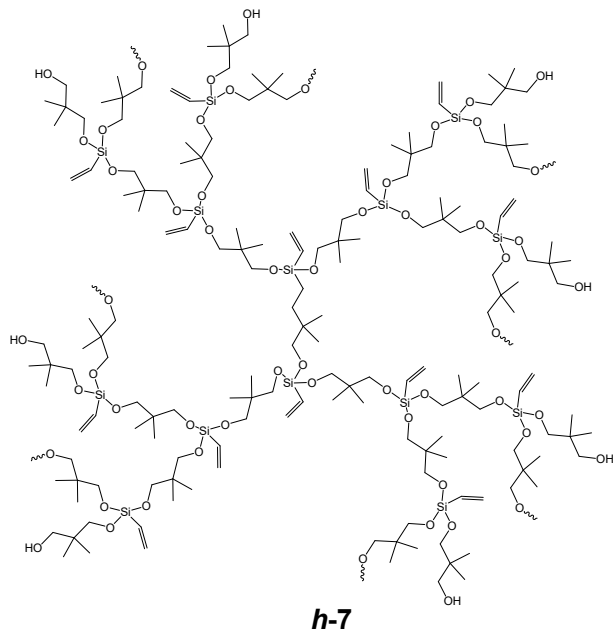
Scheme S2. Structures of the linear polysilicones (*l-1* to *l-7*).



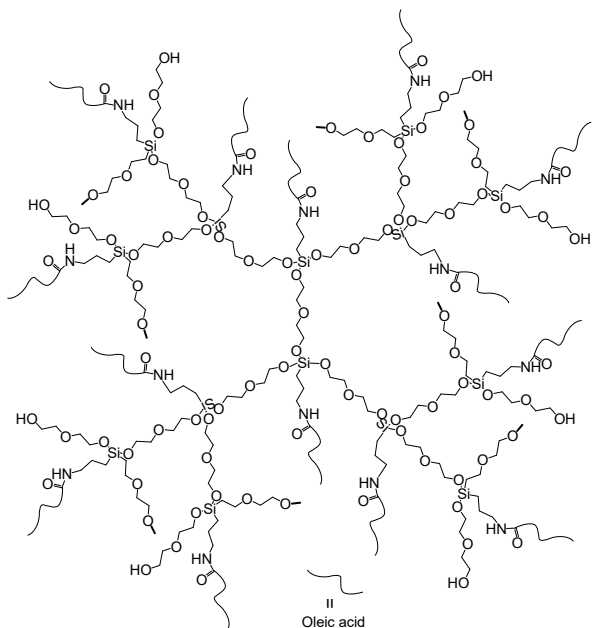
Scheme S3. Structures of the hyper-branched polysilicones (*h-1* to *h-16*).



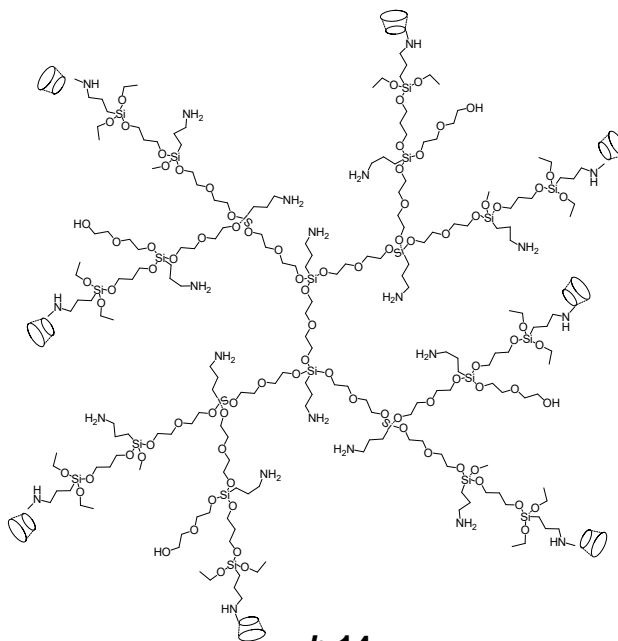
Scheme S3. Continued



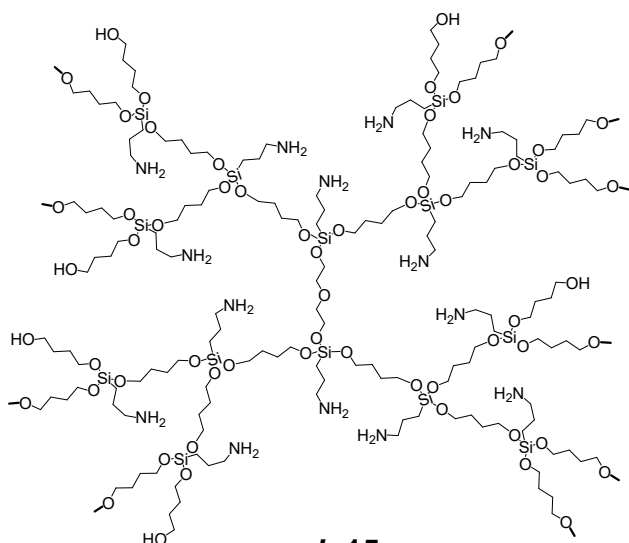
Scheme S3. Continued



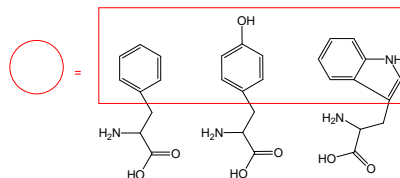
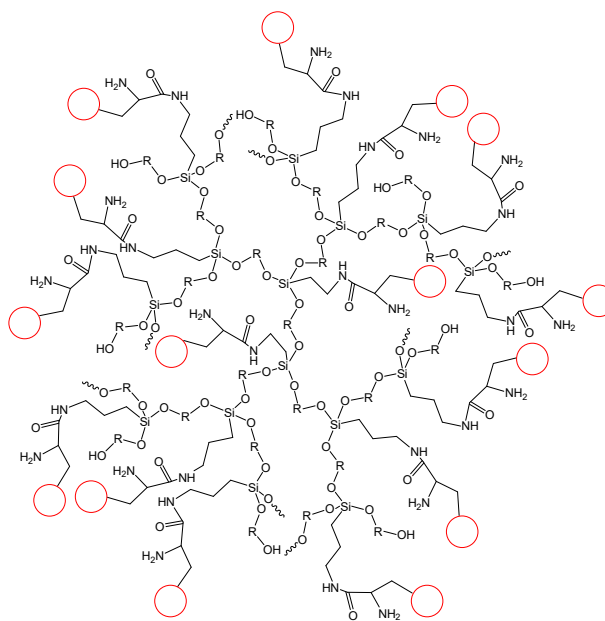
h-13



h-14

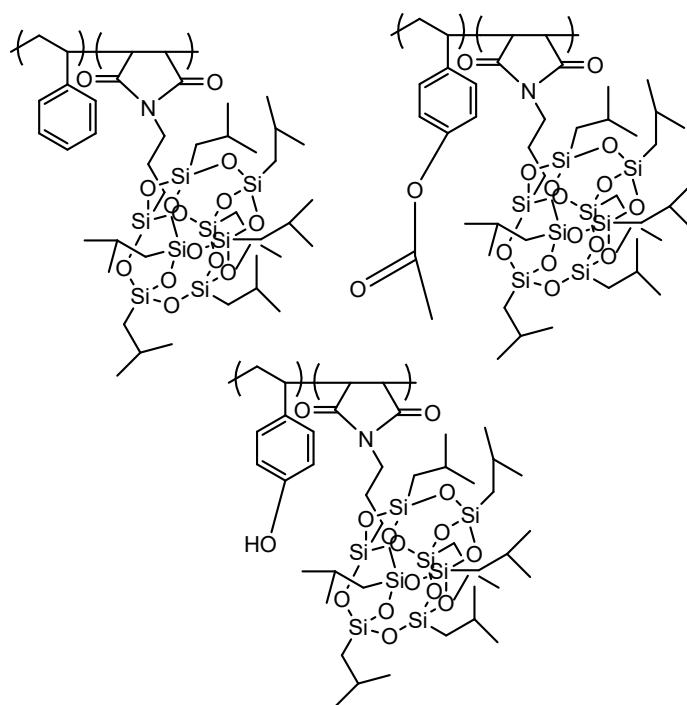


h-15



h-16

Scheme S4. Structures of the derivatives of POSS.



4. References

- 1 M.J. Rosen, Wiley, New York, 2004.
- 2 K. Sakai, S. Umezawa, M. Tamura, Y. Takamatsu, K. Tsuchiya, K. Torigoe, T. Ohkubo, T. Yoshimura, K. Esumi, H. Sakai, M. Abe, *J. Colloid Interface Sci.*, 2008, **318**, 440-448.
- 3 B. Dong, X. Y. Zhao, L. Q. Zheng, J. Zhang, N. Li, T. Inoue, *Colloids Surf. A Physicochem. Eng. Asp.*, 2008, **317**, 666-672.
- 4 G. Y. Wang, Z. P. Du, Q. X. Li, W. Zhang, *J. Phys. Chem. B*, 2010, **114**, 6872–6877.
- 5 R. Zana, *J. Colloid Interface Sci.*, 2002, **248**, 203-220.
- 6 T. Yoshimura, K. Ishihara, K. Esumi, *Langmuir*, 2005, **21**, 10409-10415.